# The Statistical Connection between Tropospheric and Stratospheric Circulation of the Northern Hemisphere in Winter

JUDITH PERLWITZ AND HANS-F. GRAF

*Max-Planck-Institut für Meteorologie, Hamburg, Germany*

(Manuscript received 17 June 1994, in final form 9 February 1995)

ABSTRACT

The associated anomaly patterns of the stratospheric geopotential height field and the tropospheric geopotential and temperature height fields of the Northern Hemisphere are determined applying the canonical correlation analysis. With this linear multivariate technique the coupled modes of variability of time series of two fields are isolated in the space of empirical orthogonal functions. The one dataset is the 50-hPa geopotential height field; the other set consists of different height fields of the tropospheric pressure levels (200, 500, 700, and 850 hPa) and the temperature of the 850-hPa pressure level. For the winter months (December, January, February) two natural coupled modes, a barotropic and a baroclinic one, of linear relationship between stratospheric and tropospheric circulation are found. The baroclinic mode describes a connection between the strength of the stratospheric cyclonic winter vortex and the tropospheric circulation over the North Atlantic. The corresponding temperature pattern for an anomalously strong stratospheric cyclonic vortex is characterized by positive temperature anomalies over higher latitudes of Eurasia. These "Winter Warmings" are observed, for example, after violent volcanic eruptions. The barotropic mode is characterized by a zonal wavenumber 1 in the lower stratosphere and by a PNA-like pattern in the troposphere. It was shown by van Loon and Labitzke that this mode can be enhanced, for example, by El Niños via the intensification of the Aleutian low.

## 1. Introduction

Investigations of observational data as well as general circulation model (GCM) studies showed a possible impact of the strength of the stratospheric winter vortex, or the polar night jet (PNJ), on the structure of tropospheric planetary waves. In context with studies of the effect of volcanic eruptions on global climate (Graf et al. 1993; Graf et al. 1994; Kodera 1994), with solar–terrestrial relationships (Kodera and Yamazaki 1990; Labitzke and van Loon 1988), as well as with GCM sensitivity studies (Boville 1984), the interrelationship between stratospheric and tropospheric circulation was studied.

A possible mechanism by which stratospheric perturbations might cause significant alterations of the tropospheric circulation was suggested, for example, in Matsuno (1970) and Hines (1974). These ideas are confirmed by results of two-dimensional linear models describing stationary wave propagation (Schmitz and Grieger 1980; Geller and Alpert 1980). They showed that changes of the stratospheric mean zonal wind influences the structure of the planetary waves and meridional heat flux in the troposphere. Tropospheric-forced ultralong vertically propagating planetary waves can be reflected at higher elevations, for example, at the PNJ, and interfere constructively or destructively with the initial waves. Consequently, alterations of the reflection properties of the lower-stratospheric zonal wind field, that is, of the zonal mean wind speed, for vertically propagating planetary waves might change amplitudes and phases of the tropospheric planetary waves and therefore change the tropospheric climate. Chen and Robinson (1992), using a three-dimensional linear time-dependent primitive equation model, found that the vertical propagation of wave activity into the stratosphere is fairly independent of the change of the zonal mean wind in the upper stratosphere, but it is very sensitive to the change of the zonal wind, especially its vertical shear, near the tropopause. In addition to the linear effects, Boville (1984) and Kodera et al. (1991), using GCMs driven by strengthened PNJ, showed some substantial nonlinear effects on the stationary as well as on the transient wave behavior.

In observations the relationship between stratospheric and tropospheric circulation is investigated under different points of view, for instance, in connection with El Niño–Southern Oscillation (ENSO), sudden warmings, and volcanoes. An atlas with point correlations of geopotential height and temperature at 30 hPa and between 30 and 500 hPa is published by Shea et al. (1992). Van Loon and Labitzke (1987)

*Corresponding author address:* Judith Perlwitz, Max-Planck-Institut für Meteorologie, Bundesstrasse 55, D-20146 Hamburg, Germany.

showed that in northern winter with warm (cold) ENSO events a weak (strong) stratospheric polar vortex and an enhanced (a weakened) Aleutian high were observed, except the winters after strong volcanic eruptions 1963/64 and 1982/83. Quiroz (1986) found a strong association of stratospheric warmings with tropospheric blockings, where blocks led by an average of 3.5 days. Case studies for strong and weak PNJ winter months (Graf et al. 1993; Kodera 1993) showed a good agreement between the results of linear models (Schmitz and Grieger 1980) and observations for the midtropospheric circulation. A considerable part of the effects therefore seems to result from the linear part of the stratosphere–troposphere interaction. The observations based on monthly data do not allow one to judge whether the troposphere or the stratosphere is the leading element in the interaction. But the abovementioned model experiments all started out from a changed stratospheric circulation influencing the tropospheric climate.

The model studies allowed an explanation of the unexpected "winter warming" in higher latitudes of Eurasia found after strong tropical volcanic eruptions by, for example, Robock and Mao (1992) and Groisman (1992). This winter warming is the result of the enhancement of a natural circulation mode by differential heating of the tropical and polar stratosphere due to the absorption of longwave radiation at the volcanic aerosol (Graf et al. 1994).

In our study, the canonical correlation analysis (CCA) is used to isolate the important coupled modes of variability between the time series of the fields of stratospheric circulation and tropospheric circulation and temperature. The CCA is a multivariate statistical analysis technique exploring the linear association between two sets of variables. We use the CCA in the phase space of the empirical orthogonal functions (EOFs) (Barnett and Preisendorfer 1987) in order to improve the signal to noise ratio. For geophysical applications Bretherton et al. (1992) showed that besides this kind of the CCA the singular-value decomposition method (SVD) is also well able to detect the coupled modes of two data fields. Whereas the singular-value decomposition of the cross-covariance matrix from two fields determines the pairs of spatial patterns that explain as much of the mean-squared temporal covariance between the two fields as possible, the CCA is a technique that maximizes the correlations of time series of two spatial patterns. This leading pair of time series is more strongly correlated than the expansion coefficients of the leading pair of patterns determined by SVD but possibly explains a smaller fraction of the covariance between the two fields (Bretherton et al. 1992). The total covariance, however, is not the best parameter to describe the relationship between two climatological fields if more processes of only a regional character are important.

The used datasets are described in section 2, and the CCA is briefly outlined in section 3. A representation and discussion of the results follows in section 4, and conclusions are given in section 5.

## 2. Data

Monthly averaged geopotential height and temperature data for different tropospheric pressure levels are used for the Northern Hemispheric region covering 20°N to the pole on a regular 5° × 5° grid. The tropospheric height fields of the 850-, 700-, 500-, and 200-hPa levels and the 850-hPa temperature data are based on the analysis of the National Meteorological Centre (NMC). The 500-hPa time series covers winter months from 1957 through 1993, while the other series were available from 1962 to 1989.

The 50-hPa height data were provided by the Stratospheric Research Group, Free University of Berlin. These data are produced from daily hemispheric analyses, mainly using radiosondes. The meridional resolution of the stratospheric grid is 10°. The grid interval is 10° longitude from 20° to 70°N and 20° longitude at 80°N. The pole point completes this grid, consisting of 235 grid points altogether. These data are used for the time period 1957–1993. Figure 1 (from Oort 1983) gives an impression of the spatial distribution of radiosonde stations, which were available in January 1971. Clearly, the concentration of stations on the Northern Hemisphere is seen, but there are only few stations in the polar areas.

In this paper the time series of the sea surface temperature index of the Southern Oscillation, as determined from tropical eastern Pacific (Wright 1989), is used for the time period 1957–1989. This time series is completed until 1993 with the NIÑO 3 sea surface temperature anomalies, published in the monthly *Climate Diagnostics Bulletin.* Here the time series of this index is abbreviated to SSTSO.

## 3. Canonical correlation analysis

The theory of CCA was developed by Hotelling (1936). Since the 1960s this technique has become a preferred analysis method in empirical social science. In meteorology the CCA was introduced by Glahn (1968). Since the end of the 1980s there have been a large number of applications, mostly in the field of climate diagnostics. Therefore, in this section only a short verbal description of the CCA follows. An exact derivation of the CCA is found, for example, in Anderson (1984).

As is mentioned in the introduction, with this technique it is possible to study the linear statistical association between two sets of variables in an optimized way. A coordinate transformation is performed in each phase space spanned by the two sets of variables, such

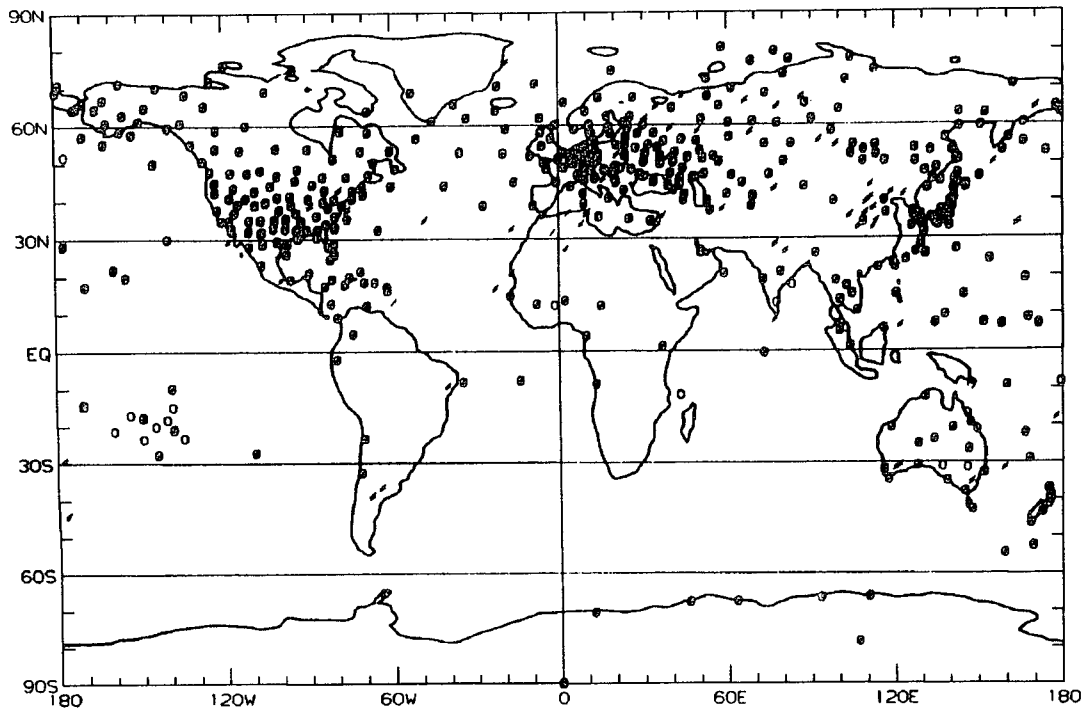


FIG. 1. Spatial distribution of radiosonde stations for January 1971 as used by Oort (1983) for their climatology. The 0000 UTC and 1200 UTC reporting stations are counted twice (figure is from Oort 1983).

that the correlation between the transformed sets of variables is maximized in pairs. The new transformed variables are called canonical variables, and the correlation coefficient of a pair of canonical variables is the canonical correlation coefficient. The pairs of canonical variables are ordered according to their canonical correlation coefficient. The pair with the maximum correlation is called the "first mode," the pair with the second highest value of the correlation coefficient is the "second mode," etc. The covariance between the original variables and their corresponding canonical variables is calculated to determine the structure of the canonical relationships.

This multivariate approach is especially useful when the interrelation between complex phenomena, which are not describable with only few variables, is to be investigated. A calculation of a multitude of bivariate and multiple correlations leads to results that may underestimate the whole interrelation. In meteorological applications, the CCA is often used to study the connection between two space–time dependent variables (Barnett and Preisendorfer 1987; Graham et al. 1987; Déqué and Servain 1989; Metz 1989; Wallace et al. 1992; Zorita et al. 1992; Barnston and Ropelewski 1992). Then the associated spatial patterns of the two datasets (often called canonical correlation patterns), determined by the calculation of the covariance between the original and the canonical variables of the sets, describes the spatial structure of the relationship. Because the canonical variables are normalized to unity, the canonical correlation patterns represent the typical strength of the signal (Zorita et al. 1992). The canonical variables are time series of weights for the associated patterns describing the strength and the sign of the patterns for each realization in time. The corresponding canonical correlation coefficient is an expression for the degree of the connection between the two sets represented by the respective canonical variables and the associated patterns. Together the canonical variables and canonical correlation patterns belonging to a canonical correlation coefficient define a coupled mode of the variability between the time series of the two data fields under consideration (Bretherton et al. 1992).

For meteorological applications, the number of gridpoint variables is often less than the number of realizations in time, and/or the spatial correlation between the variables of a data field is very high. This problem is mathematically soluble if each data field is orthogonalized by principal component analysis (PCA). If then only those principal components (PCs) explaining a considerable fraction of the total variance are used for the CCA, the number of variables is reduced and a filtering of the data eliminating noise is achieved. The mathematical description of the CCA on the basis of PCs is found in Barnett and Preisen-

dorfer (1987). In Bretherton et al. (1992) and Barnston and Ropelewski (1992) vivid graphical representations about the technique are given. Since the number of meaningful EOFs, and with it the explained fraction of the total variance of the original variables, has to be chosen, this method is influenced by a subjective factor. If the number of temporal realizations is relatively small compared to the spatial degrees of freedom, the estimation of the EOFs is uncertain, and therefore the results of the CCA are influenced by this subjectivity. Using a too large fraction of variance (near to 100%, i.e., poor filtering of the original time series) is associated with a large random error due to sampling errors. If too little variance is taken into account, it is possible that important information about the link of the two fields will be lost. Bretherton et al. (1992) suggested that a considered variance of about 70% to 80% is a good compromise between these two errors.

The significance of the canonical correlation coefficients can be tested in dependence on the number of used variables (EOFs) and the number of realizations in time. We applied the Bartlett–Lawley test (Glynn and Muirhead 1987; Kendall and Stuart 1983) of the null hypothesis that the canonical correlation coefficients $\rho_{k+1} = \cdots = \rho_p = 0$. Here $p$ and $q$ are the numbers of the used variables of the two datasets, respectively, and it is assumed that $p \leq q$. If the first $k$ correlation coefficients have been accepted as nonzero, the criterion for testing the hypothesis is

$$-\left[N - 1 - k - \frac{1}{2}(p + q + 1) + \sum_{j=1}^{k} r_j^{-2}\right] \times \ln \prod_{j=k+1}^{p} (1 - r_j^2), \quad (1)$$

which is approximately a $\chi^2$ distribution with $(p - k) \times (q - k)$ degrees of freedom. In Eq. (1) $N$ is the number of realisations, and $r_1, \ldots, r_p$ are the sample canonical correlation coefficients.

## 4. Results and discussion

### *a. Approach and preprocessing*

To investigate the interaction of stratospheric and tropospheric circulation, the canonical correlation of observed data of Northern Hemispheric geopotential heights are studied. With the CCA in the EOF space, the mean associated anomaly patterns of stratospheric and tropospheric height fields are determined in a filtered phase space. One basis set is the 50-hPa geopotential field, the other sets are different height fields of tropospheric pressure levels (200, 500, 700, and 850 hPa). The results of a further analysis is given, where the same stratospheric set is used together with the temperature of the 850-hPa layer. Later in section 4c the results of those analyses, based on the leading EOFs, which describe about 70%–75% of total variance in each field, are discussed. This in our case corresponds to three EOFs for the 50-hPa geopotential height field and eight to nine EOFs for the tropospheric fields. The canonical correlation coefficient of the discussed canonical modes are significant at least at the 99% significance level. (The test is given in section 3.) The canonical modes found are stable also if more variance is taken into account (for instance, 90% of the total variance for both the tropospheric and stratospheric fields).

The investigation is concentrated on the winter months, December, January, February, because for these months theoretical results from the literature (e.g., Charney and Drazin 1961; Matsuno 1970) allow us to expect the strongest coupling between the circulation of stratosphere and troposphere. The number of realizations is different for the individual analyses. It depends on the common available time period of the two sets of variables considered for a CCA. In each case as many realizations as possible are used. The long-term means for each of the winter months and the corresponding anomalies are calculated at each grid point. Before executing the PCA, the anomalies are weighted with the square root of the cosine of the geographic latitude to consider the area represented by the grid points. In the figures, however, this latitude weighting was not applied.

Using daily data for the analysis, the signal to noise ratio becomes so small that the analysis does not show the results as clear as with monthly means. The coupled modes do not remain stable by increasing the fraction of total variance taken into account in the CCA. The regarded region covers 20° to 90°N. A reduction of the spatial domain to, for example, 30° to 90°N does not influence the results.

### *b. EOFs of the 50-hPa geopotential height field*

In this subsection a short description of the most important EOFs of the anomalies of the Northern Hemisphere 50-hPa field is given. These EOFs explain a large fraction of the variability of the data field, and the stratospheric part of the canonical patterns resulting from all the CCAs essentially follows these EOFs.

The first EOF and the corresponding standardized PC are shown in Fig. 2a and Fig. 3, respectively. The first EOF, explaining 53% of the total variance, describes the intensity of the cyclonic stratospheric vortex in winter. This can be proved by calculation of the correlation coefficient between the PC of the first EOF and the zonally averaged zonal component of the geostrophic wind. The mean of the geostrophic zonal wind component at 65°N, 500 hPa is very highly correlated with the first PC ($r = 0.96$). Thus, the time coefficients of the first EOF determine whether the stratospheric vortex is anomalously strong (positive coefficient) or

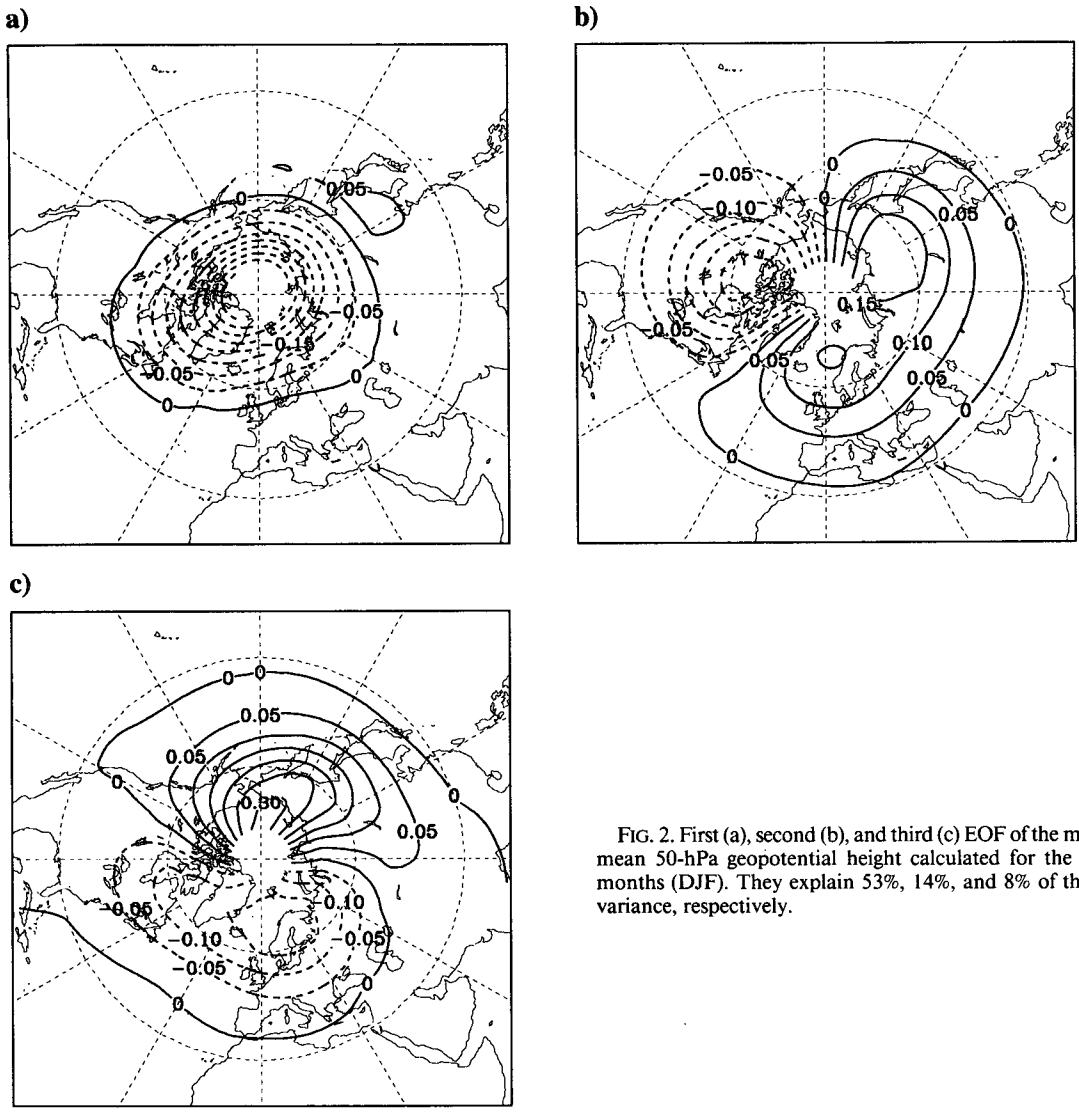


FIG. 2. First (a), second (b), and third (c) EOF of the monthly mean 50-hPa geopotential height calculated for the winter months (DJF). They explain 53%, 14%, and 8% of the total variance, respectively.

anomalously weak (negative coefficient). Because the vortex is not really zonally symmetric, the first EOF and its PC contain some more information than does the zonal wind component alone. In Fig. 3 the first PC is shown together with the time series of the SSTSO. The connection between the SSTSO and the strength of the polar night vortex was already suggested by van Loon and Labitzke (1987). For a comparison of the first PC (PC1 50 hPa) with the SSTSO, a fourfold table is given (Table 1). Provided that only the anomalies of those monthly values exceeding 0.5 standard deviation (stv) are included in the analyses (physically meaningful anomalies), the $\chi^2$-test does not show a relationship between the SSTSO and the PC1. However, an exclusion of the volcanically disturbed years (i.e., 1963/64 after Agung; 1982/83 after El Chichón; 1991/92 after Pinatubo) reduces the scatter (see numbers in bracket in Table 1) and the hypothesis of the independence of the SSTSO and the PC1 of the 50-hPa geopotential height field is refused at a confidence level of 95%.

The second and third EOFs (Figs. 2b–c), explaining 14% and 8% of the total variance, respectively, are very similar to a planetary wave of the zonal wavenumber one, but the second EOF is superimposed by a wavenumber 2. With these three EOFs, which by definition are orthogonal, it is possible to explain a large fraction (75%) of the observed variability of the monthly averaged stratospheric height field in the Northern Hemisphere winter. These EOFs characterize the

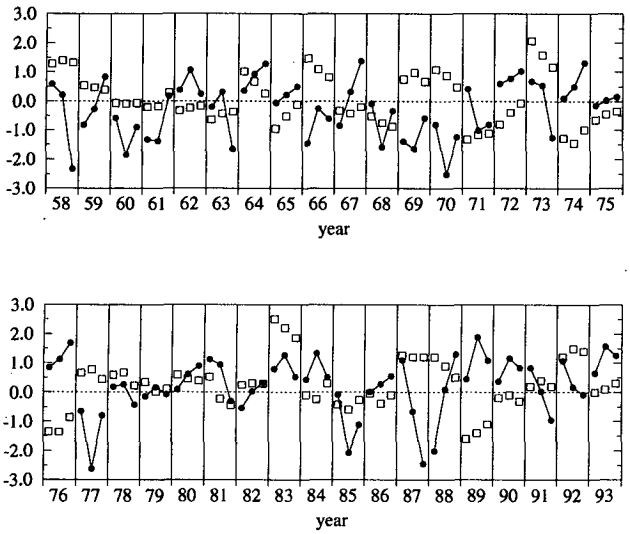


FIG. 3. First normalized principal component of the 50-hPa geopotential height field (solid lines) for the winter months DJF (corresponding to EOF in Fig. 2a) and the tropical SST-index of the SO (open squares). Year is indicated for JF.

strength of the vortex and its disturbance by waves of wavenumbers 1 and 2.

The tropospheric EOFs will not be discussed here in detail because these can be estimated only roughly. The smaller-scale phenomena occurring in the troposphere lead to a smoother distribution of explained variance over the EOFs than was found in the stratosphere. Estimations of EOFs of tropospheric Northern Hemispheric geopotential height fields can be found in Wallace and Gutzler (1981) and Barnston and Livezey (1987).

### c. *Results of the CCA*

#### 1) TROPOSPHERIC GEOPOTENTIAL HEIGHT

The study was performed for the geopotential heights of the 850-, 700-, 500-, and 200-hPa layers. We shall concentrate here on the 500-hPa layer results since the time series are longest for this layer. For this analysis the months of the winters 1957/58 to 1992/93 (108 realizations) are used. The canonical correlation patterns of the three modes of the 50-hPa heights essentially follow the first three EOFs. The canonical correlation coefficient of the first canonical mode is equal to 0.70. The pair of associated patterns of this mode (Figs. 4a and 4c) explain 42% (16%) of the total variance of the 50-hPa (500-hPa) geopotential height field. Figures 4b and 4d show the local variance at the individual grid points explained by the corresponding first canonical variables in our time interval. For the sake of clarity, in Figs. 4b and 4d the isolines of explained local variance of less than 20% are omitted. Whereas the first canonical correlation pattern of the stratospheric field describes a global-scale signal, the tropospheric signal has a more regional character. The stratospheric pattern clearly is a measure of the strength of the polar stratospheric vortex, with more than 80% of the total variance being explained right over the North Pole. However, there are only some regions over the Northern Hemisphere where more than 20% of the local variance of the 500-hPa field is explained. These regions are concentrated over the North Atlantic. The strongest signal appears over the North American archipelago, the Davis Strait, and Greenland, where up to 70% of the total variance is explained. Smaller spots with up to 30% of explained variance occur over the midlatitudes in the western North Atlantic, over Western Europe, and in far eastern Asia.

The first pair of associated canonical patterns describes a relationship between the stratospheric and the tropospheric circulation that was already found with simple linear model studies (e.g., Grieger and Schmitz 1984). The associated patterns are very similar to the leading mode of the SVD analysis between 50- and 500-hPa geopotential heights, found by Baldwin et al. (1994). An anomalously intensive cyclonic vortex in the lower stratosphere is connected with a change of the tropospheric circulation over the whole North Atlantic (positive time coefficients of the canonical variables). The trough normally occurring downwind of the Rocky Mountains is strengthened and shifted somewhat to the east. Thus, over the western North Atlantic a more zonal circulation develops, and over the eastern North Atlantic a southwesterly component of the tropospheric circulation is enhanced. In general the associated patterns of the first canonical mode of geopotential anomalies are similar throughout the troposphere. In Fig. 5 the tropospheric part of the associated patterns and its pattern of explained local variances of the first canonical mode of the CCA of the 50- and 850-hPa geopotential fields are shown. The Greenland trough is associated with some baroclinic effects, leading to a westward shift of the trough axis with the height. While the trough is centered over East Greenland in the lower troposphere, it lies over the Davis Strait in the upper troposphere. This circulation anomaly is then connected with temperature anomalies as described in Graf et al. (1994). The baroclinic char-

TABLE 1. Fourfold table for the first PC of the 50-hPa layer (PC1 50 hPa) versus the SSTSO, as defined in text. [Only values exceeding ±0.5 standard deviations (stv) are counted.]

| | PC1 50 hPa | |
|---|---|---|
| SSTSO | $< -0.5$ stv | $>0.5$ stv |
| $>0.5$ stv | 14 | 9 (4) |
| $< -0.5$ stv | 7 | 10 |

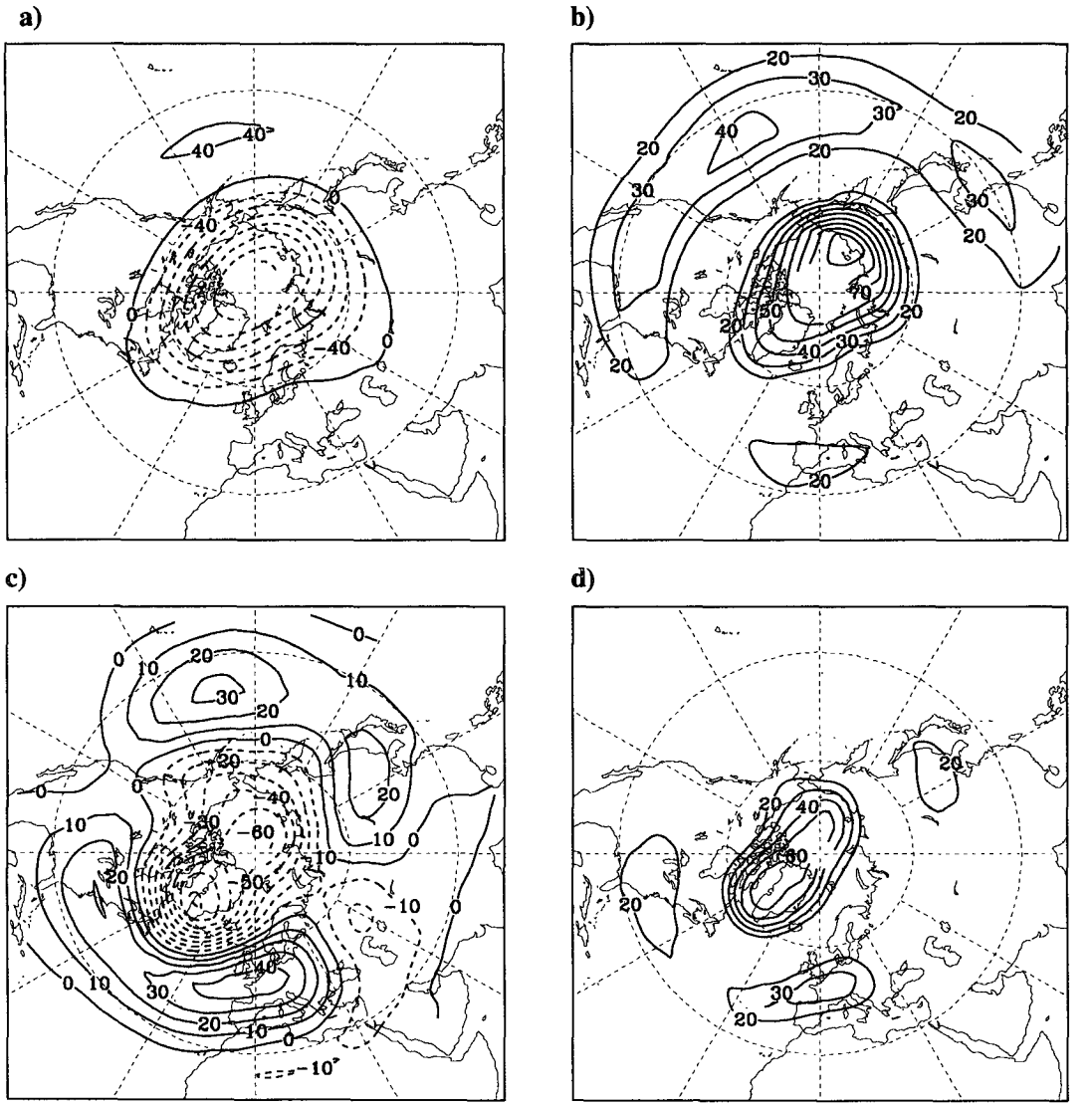


FIG. 4. *Left panels:* Associated patterns of the first canonical mode of the 50-hPa geopotential height field (a) contour interval: 40 gpm, and the 500-hPa geopotential height field (c) contour interval: 10 gpm. *Right panels:* Patterns of percent of local variance (contour interval: 10%, starting at 20%) explained by the pair of the canonical variables of the first canonical mode in their corresponding original data fields (b) 50-hPa geopotential height field, (d) 500-hPa geopotential height field.

acter of the mode also becomes evident from the temperature analysis in section 4c(2).

With a strong stratospheric vortex, a positive geopotential anomaly over East Asia is also observed. An anomalously weak stratospheric vortex on the other hand is connected with an anomalously weak North American trough, diminished westerly winds over the North Atlantic, and a negative tropospheric geopotential height anomaly over East Asia (negative time coefficients of the canonical variables). In Fig. 6 these time series of the canonical variables giving the weights of the above described anomaly patterns for the individual winter months are shown. The good correlation of the canonical variables ($r = 0.70$) is seen, and the relationship described above is not dominated by few single (high loaded) realizations. The benefit of the CCA is that it depicts linear relationships independent on its causes. Therefore, it is not necessary to know in advance which processes (e.g., QBO, solar activity, volcanoes, etc.) are responsible for the relation like for the calculation of composites. The canonical variables depending on time can be compared with well-defined single events.

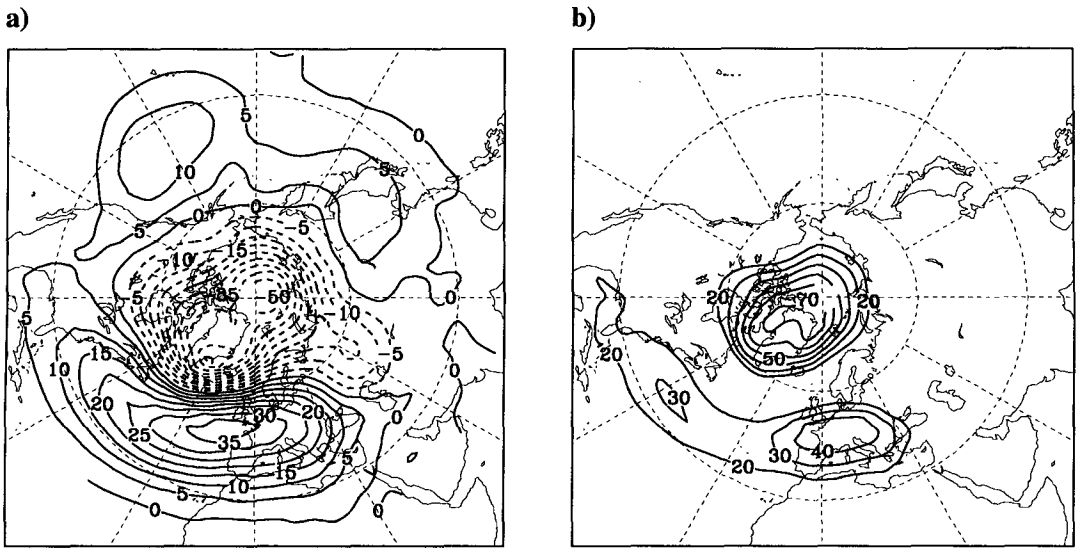


FIG. 5. (a) Tropospheric part of the associated patterns of the first canonical mode of the CCA of the 50-hPa geopotential field and the 850-hPa geopotential height field (contour interval: 5 gpm), and (b) corresponding pattern of percent of local variance (contour interval: 10%, starting at 20%) explained by their canonical variable.

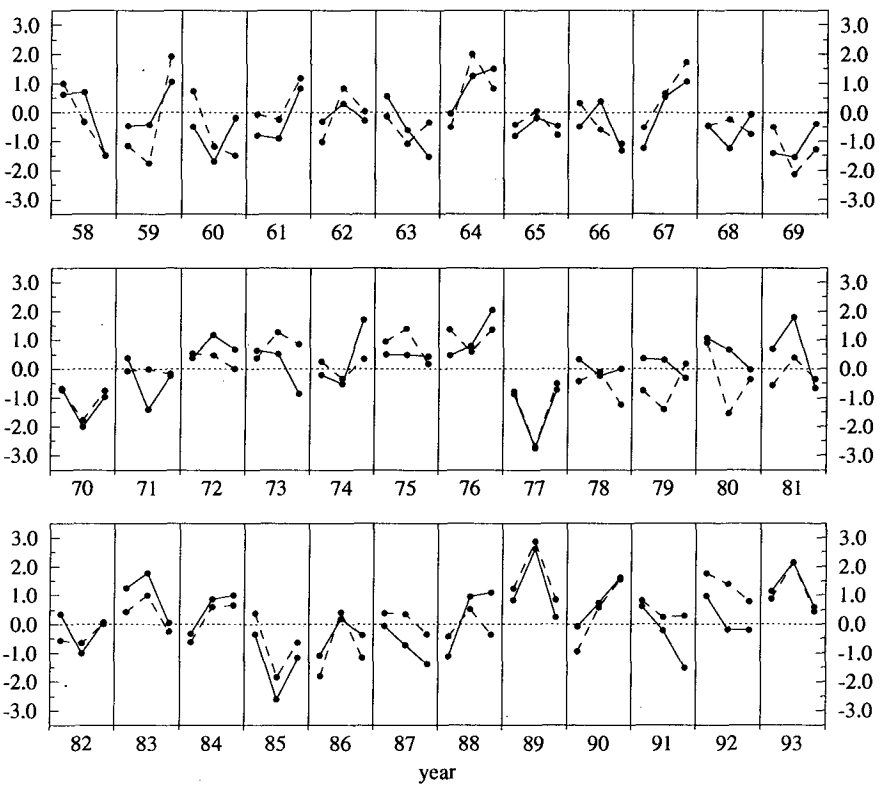


FIG. 6. Pair of canonical variables of the first canonical mode of the CCA of the 50-hPa geopotential height field (solid lines) and the 500-hPa geopotential height field (dashed lines). The CCA is applied only on the winter months DJF (year is indicated for JF).

The associated patterns and the explained local variances of the second canonical mode, characterized by essentially the same value of the canonical correlation coefficient ($r = 0.68$) as the first mode, are shown in Fig. 7. The stratospheric canonical correlation pattern is characterized by a zonal wavenumber one, much like the second EOF (Fig. 2b) with extremes over North America and West Siberia. At these places also the highest values of explained local variance appear (Fig. 7a). The tropospheric part of the associated patterns (Fig. 7c) depicts a Pacific–North America Oscillation (Wallace and Gutzler 1981). These patterns do not show any horizontal shift throughout the troposphere. Obviously they depict a barotropic mode (see also the temperature analysis below). In the troposphere, there are no significant anomalies found over Eurasia. The tropospheric explained local variance in Fig. 7d has the highest value in the Aleutian low area (>50%), the other two centers of suggestive values being over the central North Pacific and over the Great Plains.

Positive (negative) values of the canonical variable (Fig. 8) of the second mode mean that in the midtroposphere a weak (strong) Aleutian low is flanked by negative (positive) geopotential height anomalies over the central North Pacific and over large parts of North America.

For the second mode there exist correlations, which are significantly different from zero at the 95% confidence level, between the SSTSO and both the stratospheric ($r = -0.35$) and the tropospheric ($r = -0.44$)

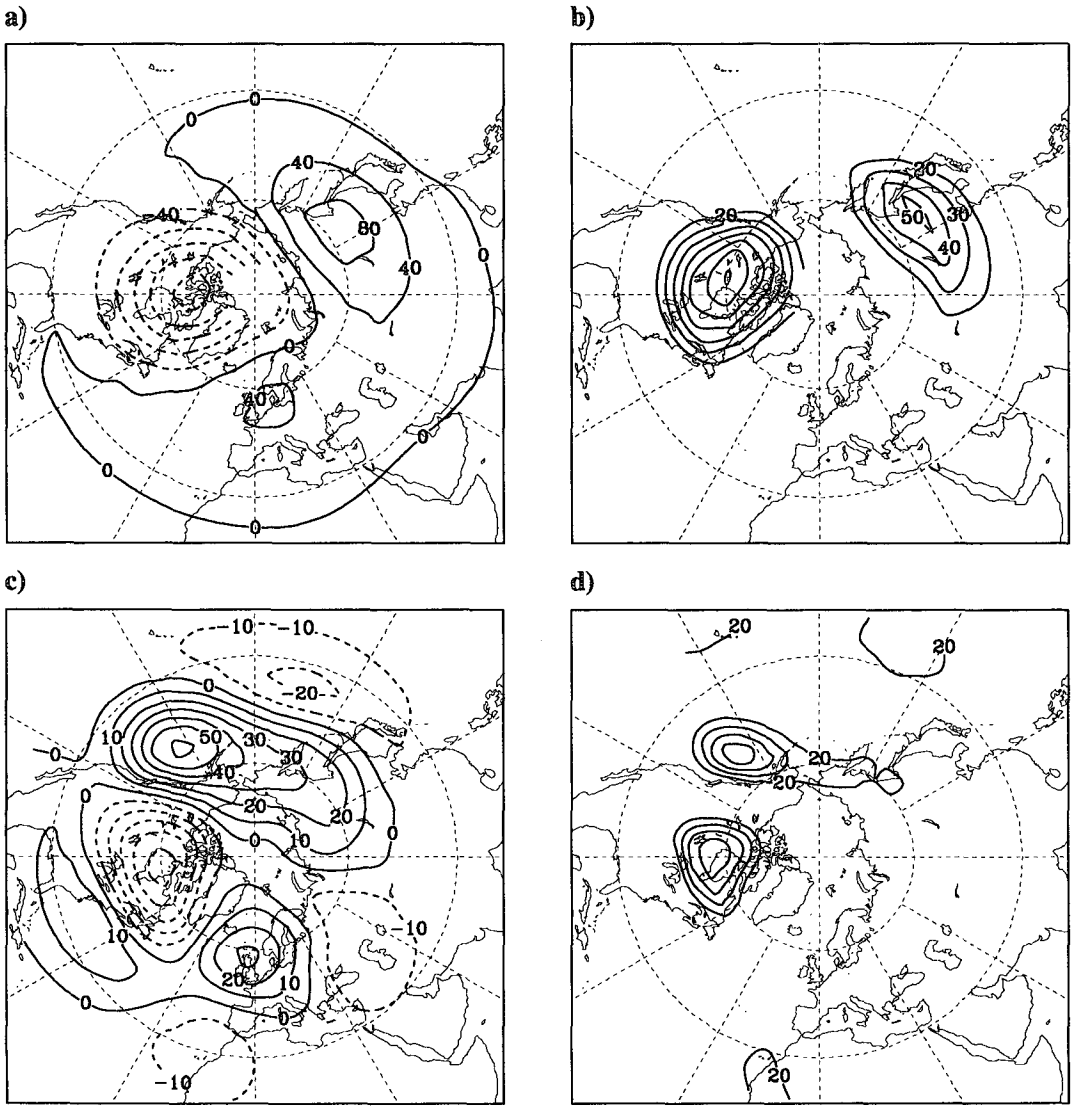


FIG. 7. As Fig. 4 but for the second canonical mode.

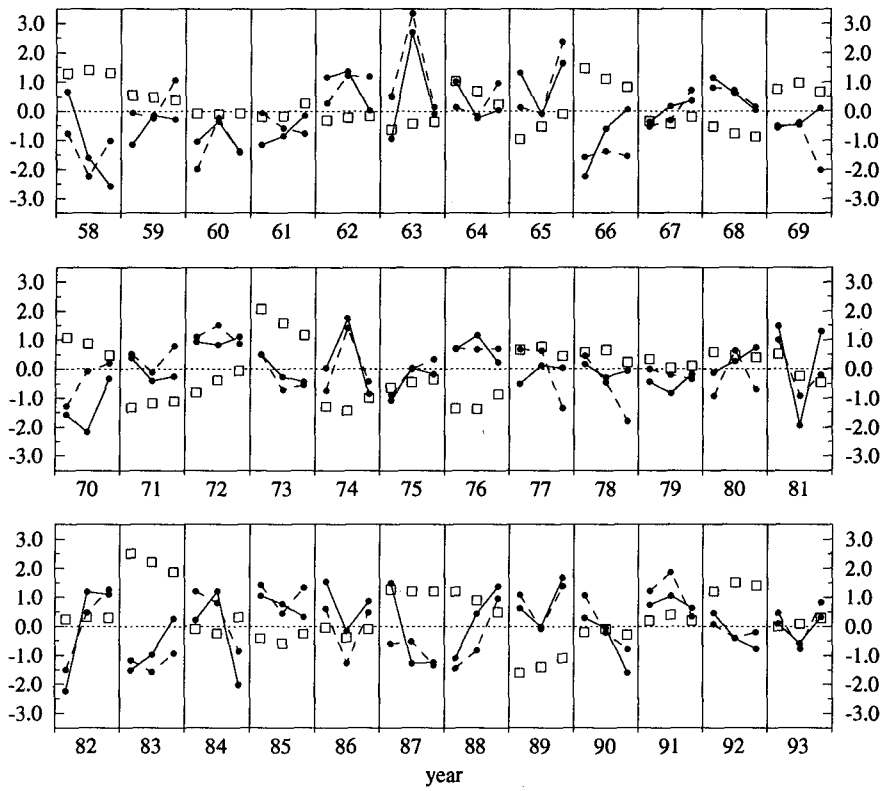


FIG. 8. Pair of canonical variables of the second canonical mode of the CCA of the 50-hPa geopotential height field (solid lines) and the 500-hPa geopotential height field (dashed lines) and the tropical SST-index of the SO (open squares). The CCA is applied only on the winter months DJF (year is indicated for JF).

canonical variables (Fig. 8). In the case of El Niños (excluding those accompanied by strong explosive volcanic eruptions) 12 (13) out of the 18 winter months have negative weights of the stratospheric (tropospheric) canonical variable; that is, they are associated with positive height anomalies over central North America and negative anomalies over the North Pacific. Additionally, for a comparison of the SSTSO with the canonical variables of the second mode (CV2), two fourfold tables are given (Table 2), one for each time series (left table for the CV2 of the 50-hPa layer; right table for the CV2 of the 500-hPa layer). Again, provided that only the anomalies of those monthly values exceeding 0.5 stv are included in the analyses, the $\chi^2$-tests for both fourfold tables show that the hypothesis of independence of the SSTSO and the canonical variables is refused at a confidence level of 99%. This relationship between the phase of the PNA and the SST in the eastern tropical Pacific was shown in Horel and Wallace (1981).

As can easily be determined from the time series (Fig. 6 and Fig. 8), both canonical modes can have high loading even without any known external forcing (e.g., El Niño or volcanic eruptions of Agung in 1963, El Chichón in 1982, and Pinatubo in 1991). Therefore we call them natural associated modes.

### 2) TEMPERATURE OF 850-hPa LAYER

In terms of climate variability, the temperature of the lower troposphere is the most interesting parameter to the public. Thus, we also performed an analysis of the canonical correlation between the stratospheric geopotential heights and temperatures of the 850-hPa layer.

The first canonical mode (canonical correlation coefficient: 0.71) of the associated patterns of the 50-hPa geopotential height anomalies (Fig. 9a) and the 850-hPa temperature (Fig. 9c) corresponds to the second mode of the geopotential CCA, discussed in section 4c(1). The stratospheric canonical correlation pattern (Fig. 9a) is again very similar to the second EOF (Fig. 2b). The difference from the result of CCA with tropospheric height fields is a deeper North American low. As can be seen from Fig. 9d, the area with substantially explained variance of the tropospheric temperature is mainly the central part of North America north of 40°N, where up to 50% of local variance is explained.

TABLE 2. Two fourfold tables for the two variables of the second canonical mode (CV2 50 hPa and CV2 500 hPa) versus the SSTSO, respectively, as defined in text. [Only values exceeding ±0.5 standard deviations (stv) are counted.]

| CV2 50 hPa | | | CV2 500 hPa | | |
|---|---|---|---|---|---|
| SSTSO | < −0.5 stv | >0.5 stv | SSTSO | < −0.5 stv | >0.5 stv |
| >0.5 stv | 14 | 3 | >0.5 stv | 20 | 3 |
| < −0.5 stv | 4 | 13 | < −0.5 stv | 5 | 16 |

Two further areas with suggestive values of explained variance are situated in the Northeast Pacific and over East Siberia. The main feature of the association of stratospheric geopotential and lower-tropospheric temperature is the North America anomaly. This feature obviously is a barotropic phenomenon. It can be

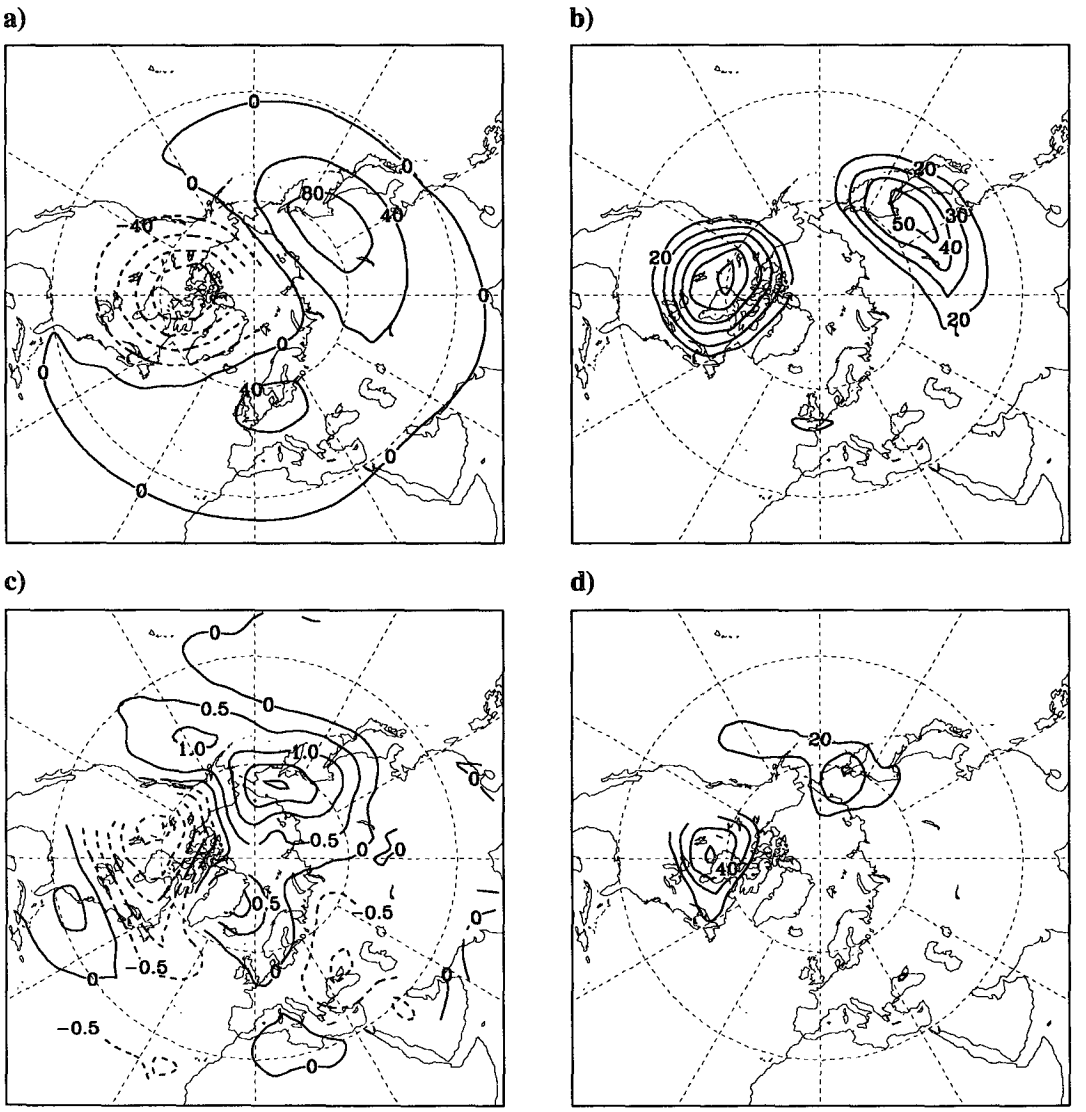


FIG. 9. *Left panels:* Associated patterns of the first canonical mode of the 50-hPa geopotential height field (a), contour interval: 40 gpm, and 850-hPa temperature field (c), contour interval: 0.5 K. *Right panels:* Patterns of percent of local variance (contour interval: 10%, starting at 20%) explained by the pair of the canonical variables of the first canonical mode in their corresponding original data fields (b) 50-hPa geopotential height field, (d) 850-hPa temperature field.

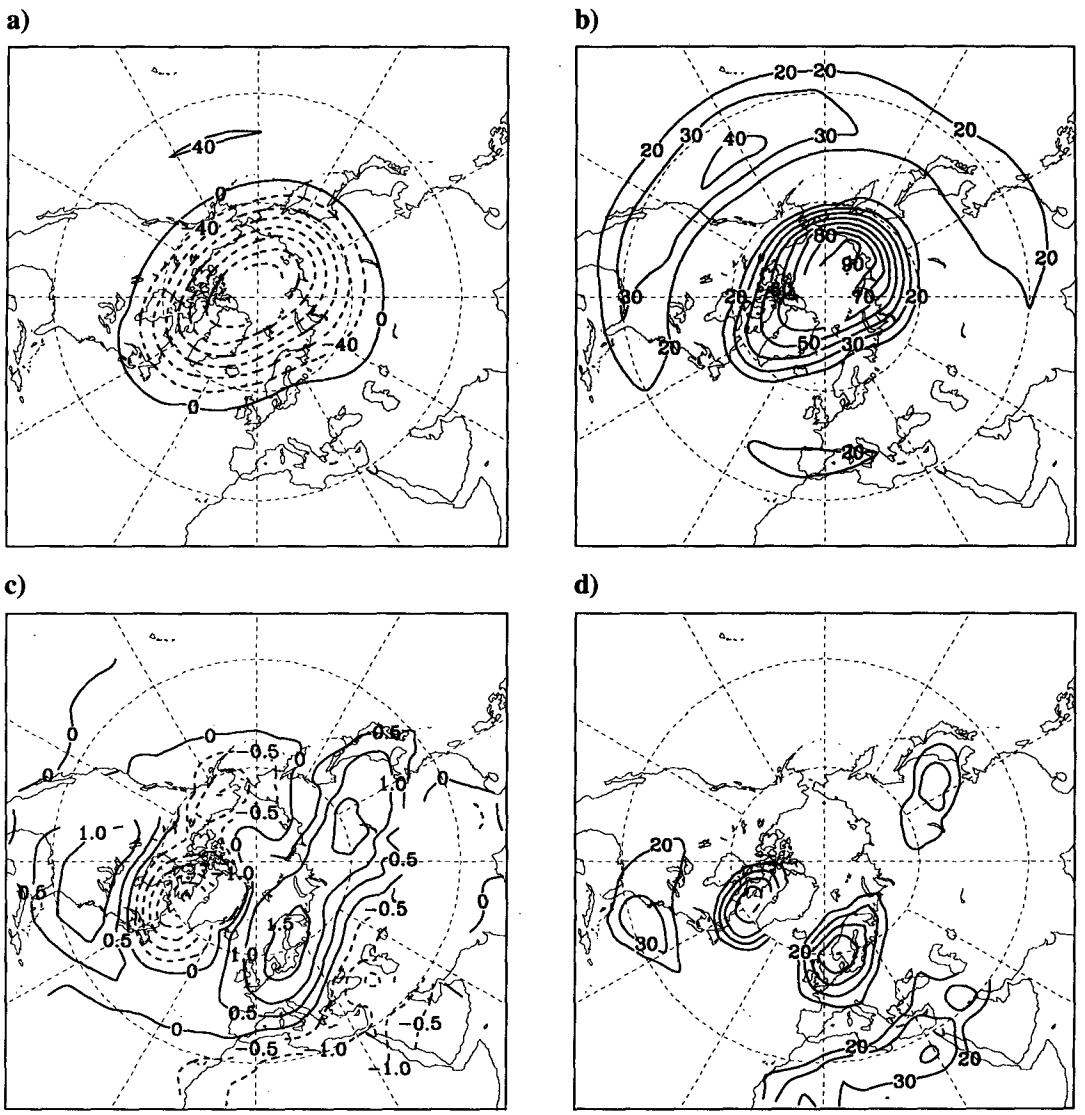


FIG. 10. As Fig. 9 but for the second canonical mode.

traced throughout the whole troposphere (not shown here) without any local shifts between temperature and geopotential anomaly patterns.

The tropospheric temperature anomaly pattern (Fig. 10c) of the second canonical mode is similar to the patterns Graf et al. (1994) found with a simple selection of strong and weak polar winter vortexes. The canonical correlation coefficient of this mode is equal to 0.64, and 44% (12%) of the total variance is explained by the stratospheric (tropospheric) part of associated patterns. The stratospheric canonical correlation pattern (Fig. 10a) corresponds to the first EOF. In the tropospheric temperature field, most of the local variance can be explained over the North Atlantic and adjacent continental areas. The highest values (50%) are found over the Davis Strait and over the North Sea and western Scandinavia (Fig. 10b). The associated patterns suggest positive (negative) lower-tropospheric temperature anomalies in case of a strong (weak) polar winter vortex over northern Eurasia and cold (warm) conditions over Northwest America to Greenland. As was outlined previously (Graf et al. 1994), these temperature anomalies are mainly due to advective processes. The baroclinicity associated with these processes can be seen from a comparison of Fig. 5a (geopotential anomalies) and Fig. 10c (temperature anomalies). Clearly, a different horizontal structure appears for the 850-hPa layer over the North Atlantic, with the geopotential centers over Greenland and Northwest

Europe and the temperature anomaly centers over Davis Strait and North Europe.

## 5. Conclusions

Applying the canonical correlation analysis technique to stratospheric geopotential and tropospheric geopotential fields and the 850-hPa temperature field of the Northern Hemisphere for a 36-yr (1957/58–1992/93; 500-hPa geopotential height) or 27-yr (1962/63–1988/89; 200-, 700-, 850-hPa geopotential height, 850-hPa temperature) period of winter months, two natural modes were found. These modes associate geopotential height anomalies in the Northern Hemisphere winter stratosphere with circulation and temperature anomalies in the troposphere. The method applied does not allow any statements about cause and effect. The order of the modes is determined by the canonical correlation coefficient. Both modes have comparable canonical correlation coefficients. A more distinct difference was found in the vertical structure of the tropospheric part of the mode. Here we found one mode that is more baroclinically influenced in the troposphere. This mode is associated with the strength of the polar winter vortex in the stratosphere. The mode describing a zonal wavenumber one in the stratosphere is associated with barotropic features in the troposphere. In the troposphere this barotropic mode shows a pattern much like the PNA. The investigation of the canonical variables shows a connection between the strength of the barotropic mode and El Niño events. During El Niños a strengthened Aleutian low and positive geopotential height anomalies over North America (positive PNA-Index) are connected with a zonal wavenumber one structure in the stratosphere with a ridge over North America and a trough over East Asia. Model experiments with prescribed sea surface temperature anomalies of the El Niño type (Kirchner and Graf 1993) showed that this natural mode may be driven by the tropospheric anomalies. The baroclinic mode, however, was enhanced in model studies (Boville 1984; Kodera et al. 1991; Graf et al. 1994) from the stratosphere. This mode is determined by a strong polar night vortex in the stratosphere, which besides natural variability can be forced by low-latitude volcanic aerosols. The strongest tropospheric effects in this case are found over the North Atlantic in the geopotential field with strengthened westerlies leading to positive temperature anomalies over northern Eurasia. The strong negative temperature anomalies in the east of North America are due to the advection of polar air at the windward side of the Greenland trough.

Labitzke and van Loon (1991) showed that there exists a negative trend in the area-weighted annual mean 50-hPa temperature of the Northern Hemisphere (10°N–90°N). They also found a positive trend in the annual mean area-weighted height of the pressure surface layers of the lower stratosphere (Labitzke and van Loon 1994). This is consistent with the influence of, for example, greenhouse gas effects of tropospheric variations on the lower-stratospheric pressure layers. We calculated the trends of the zonal mean height of the 50-hPa geopotential layer for different latitudes. And we find in winter the trends are positive only south of 60°N. In Figs. 11a and 11b for selected latitudes (30°, 70°N) the time series are given together with the linear trend function (note that the scale of the ordinate is larger north of the polar circle because of the increased variability in this area). The $t$ test value for the linear regression coefficient describing the trend is given as well. With 36 degrees of freedom, a $t$ test value of 2.03 determines the 95% significance threshold. The term trend here means a change of the mean value of the data with time, tested against the noise. Thus, a significant trend may also be part of a long-term oscillation of the climate, which because of the shortness of the time series cannot be tested. This means that the positive trends between 20° and 40°N are statis-

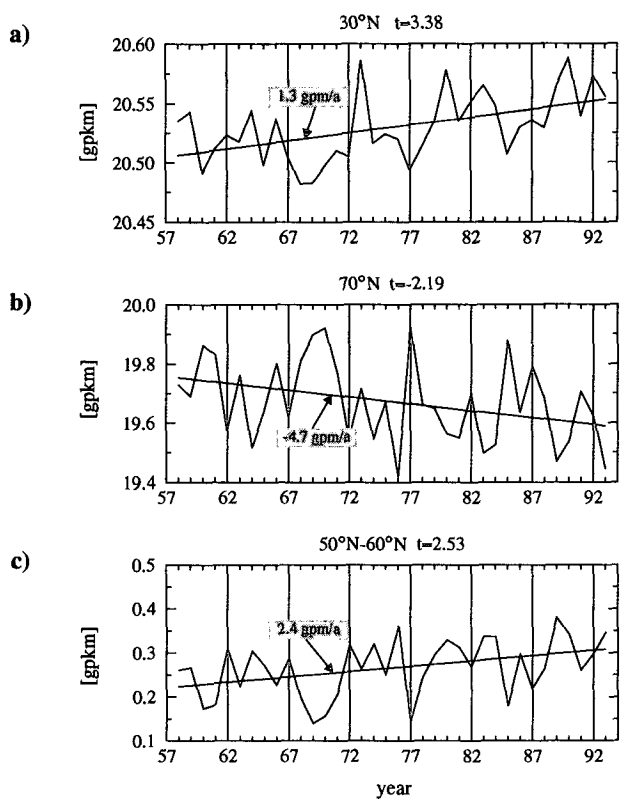


FIG. 11. (a) Winter mean (DJF) time series (1957/58–1992/93) of the zonally averaged 50-hPa geopotential height together with the linear trend function for 30°N. (b) Same as in (a) but for 70°N. (c) Time series of the difference of the winter mean (DJF) zonally averaged 50-hPa geopotential height between 50° and 60°N together with the linear trend function (t: $t$ test value for the linear regression coefficient).

tically significant as well as the negative trend at 70°N. Between 50° and 60°N the trend changes sign. This implies a strengthening of the PNJ due to the increased meridional temperature gradient near the polar circle. In Fig. 11c the height difference of the 50-hPa layer between 50° and 60°N is displayed giving evidence of the statistically significant intensification of the PNJ. Here we discussed the results based on the original time series. The computation of the canonical modes based on the detrended data does not show any remarkable difference.

Kodera and Yamazaki (1994) discussed the effect of the cooling trend of the polar stratosphere in winter on the tropospheric circulation. Based on our geopotential trend analysis for the lower stratosphere, we suggest that an indirect greenhouse effect is responsible for the polar cooling. The increase of tropospheric temperature in lower latitudes due to combined greenhouse gas effects leads to an initial intensification of the polar winter vortex by lifting the geopotential height layers. The intensified vortex then causes polar cooling because the transport of heat to polar latitudes by planetary waves is reduced and parcels inside the vortex remain in the shadow during the polar night, thereby cooling toward the radiation equilibrium. This enhanced polar cooling in a positive feedback loop strengthens the vortex. The dynamic coupling between stratospheric and tropospheric winter circulation, described by our baroclinic mode, is then responsible for positive temperature anomalies over the continents in northern middle and high latitudes (Graf et al. 1994).

*Acknowledgments.* We wish to express our sincere thanks to the Stratospheric Research Group of Prof. Karin Labitzke from the Free University of Berlin, who supplied the data to us. Thanks are also due to Dr. G. Schmitz and V. Kharin for their interest and valuable discussion. We thank Dr. John E. Janowiak from Climate Analysis Center for the update of the NMC monthly 500-hPa geopotential heights of the Northern Hemisphere and the unknown reviewers for the constructive suggestions to improve the paper. This work in part was sponsored by Contract 07-KFT-86/2 by the Bundesministerium für Forschung und Technologie.

## REFERENCES

Anderson, C. W., 1984: *An Introduction to Multivariate Statistical Analysis.* 2d ed., Wiley & Sons, 675 pp.

Baldwin, M. P., X. Cheng, and T. J. Dunkerton, 1994: Observed correlations between winter-mean tropospheric and stratospheric circulation anomalies. *Geophys. Res. Lett.*, **21,** 1141–1144.

Barnett, T. P., and R. Preisendorfer, 1987: Origins and levels of monthly and seasonal forecast skill for United States surface air temperatures determined by canonical correlation analysis. *Mon. Wea. Rev.*, **115,** 1825–1850.

Barnston, A. G., and R. E. Livezey, 1987: Classification, seasonality, and persistence of low-frequency atmospheric circulation patterns. *Mon. Wea. Rev.*, **115,** 1083–1126.

——, and C. F. Ropelewski, 1992: Prediction of ENSO episodes using canonical correlation analysis. *J. Climate,* **5,** 1316–1345.

Boville, B. A., 1984: The influence of the polar night jet on the tropospheric circulation in a GCM. *J. Atmos. Sci.*, **41,** 1132–1142.

Bretherton, C. S., C. Smith, and J. M. Wallace, 1992: An intercomparison of methods for finding coupled patterns in climate data. *J. Climate,* **5,** 541–560.

Charney, J. G., and P. G. Drazin, 1961: Propagation of planetary-scale disturbances from the lower into the upper atmosphere. *J. Geophys. Res.*, **66,** 83–109.

Chen, P., and W. A. Robinson, 1992: Propagation of planetary waves between the troposphere and stratosphere. *J. Atmos. Sci.*, **49,** 2533–2545.

Déqué, M., and J. Servain, 1989: Teleconnections between tropical Atlantic sea surface temperatures and midlatitude 50-kPa heights during the period 1964–86. *J. Climate,* **2,** 929–944.

Geller, M. A., and J. C. Alpert, 1980: Planetary wave coupling between the troposphere and the middle atmosphere as a possible sun-weather mechanism. *J. Atmos. Sci.*, **37,** 1197–1215.

Glahn, H. R., 1968: Canonical correlation analysis and its relationship to discriminant analysis and multiple regression. *J. Atmos. Sci.*, **25,** 23–31.

Glynn, W. J., and R. J. Muirhead, 1987: Inference in canonical correlation analysis. *J. Multivariate. Anal.*, **8,** 469–478.

Graf, H.-F., I. Kirchner, A. Robock, and I. Schult, 1993: Pinatubo eruption winter climate effects: Model versus observations. *Climate Dyn.*, **9,** 81–93.

——, J. Perlwitz, and I. Kirchner, 1994: Northern Hemisphere tropospheric midlatitude circulation after violent volcanic eruptions. *Contrib. Atmos. Phys.*, **67,** 3–13.

Graham, N. E., J. Michaelsen, and T. P. Barnett, 1987: An investigation of the El Niño–Southern Oscillation cycle with statistical models. Part 1. Predictor field characteristics. *J. Geophys. Res.*, **92,** 14 251–14 270.

Grieger, N., and G. Schmitz, 1984: The Northern Hemisphere stationary planetary waves and associated Eliassen–Palm cross-sections of the stratosphere and mesosphere. *Z. Meteor.*, **34,** 341–353.

Groisman, P. Y., 1992: Possible regional climate consequences of the Pinatubo eruption: An empirical approach. *Geophys. Res. Lett.*, **19,** 1603–1606.

Hines, C. O., 1974: A possible mechanism for the production of sun-weather correlations. *J. Atmos. Sci.*, **31,** 589–591.

Horel, J. D., and J. M. Wallace, 1981: Planetary-scale atmospheric phenomena associated with the Southern Oscillation. *Mon. Wea. Rev.*, **109,** 813–829.

Hotelling, H., 1936: Relations between two sets of variates. *Biometrika,* **28,** 321–377.

Kendall, M. G., and A. Stuart, 1983: *The Advanced Theory of Statistics.* Vol. III, 4th ed., Charles Griffin, 780 pp.

Kirchner, I., and H.-F. Graf, 1993: Volcanos and El Niño-signal separation in winter. MPI-Report-No. 107, Max-Planck-Institut für Meteorologie, FRG, 57 pp.

Kodera, K., 1993: Influence of the stratospheric circulation change on the troposphere in the Northern Hemisphere winter. *The Role of the Stratosphere in Global Change.* M. L. Chanin, Ed., Springer Verlag, 227–243.

——, 1994: Influence of volcanic eruptions on the troposphere trough stratospheric dynamical processes in the Northern Hemisphere winter. *J. Geophys. Res.*, **99,** 1273–1282.

——, and K. Yamazaki, 1990: Long-term variation of upper stratospheric circulation in the Northern Hemisphere in December. *J. Meteor. Soc. Japan,* **68,** 101–105.

——, and ——, 1994: A possible influence of recent polar stratospheric coolings on the troposphere in the Northern Hemisphere winter. *Geophys. Res. Lett.*, **21,** 809–812.

——, M. Chiba, K. Yamazaki, and K. Shibata, 1991: A possible influence of the polar night stratospheric jet on the subtropical tropospheric jet. *J. Meteor. Soc. Japan,* **69,** 715–721.

Labitzke, K., and H. van Loon, 1988: Association between the 11-year solar cycle, the QBO, and the atmosphere. Part I: The troposphere and the stratosphere in the Northern Hemisphere in winter. *J. Atmos. Terr. Phys.*, **50,** 197–206.

——, and ——, 1991: Some complications in determined trends in the stratosphere. *Adv. Spac. Res.*, **11,** 321–330.

——, and ——, 1994: A note on trends in the stratosphere: 1958–1992. *COSPAR Colloquia Series, 5,* 537–546.

van Loon, H., and K. Labitzke, 1987: The Southern Oscillation. Part V: The anomalies in the lower stratosphere of the Northern Hemisphere in winter and a comparison with the quasi-biennial oscillation. *Mon. Wea. Rev.*, **115,** 357–369.

Matsuno, T., 1970: Vertical propagation of stationary planetary waves in the winter Northern Hemisphere. *J. Atmos. Sci.*, **27,** 871–883.

Metz, W., 1989: Low-frequency anomalies of atmospheric flow and the effects of cyclone-scale eddies: A canonical correlation analysis. *J. Atmos. Sci.*, **46,** 1026–1041.

Oort, A. H., 1983: Global atmospheric circulation statistics, 1958–1973. *NOAA Professional Paper, 14,* U.S. Government Printing Office, Washington, D.C., 180 pp. + 47 microfiches.

Quiroz, R. S., 1986: The association of stratospheric warmings with tropospheric blocking. *J. Geophys. Res.*, **91,** 5277–5285.

Robock, A., and J. Mao, 1992: Winter warming from large volcanic eruptions. *Geophys. Res. Lett.*, **12,** 2405–2408.

Schmitz, G., and N. Grieger, 1980: Model calculations on the structure of planetary waves in the upper troposphere and lower stratosphere as a function of the wind field in the upper stratosphere. *Tellus,* **32,** 207–214.

Shea, D. J., H. van Loon, and K. Labitzke, 1992: Point correlations of geopotential height and temperature at 30 mb and between 500 mb and 50 mb. NCAR Tech. Note, NCAR/TN-268+STR, 293 pp.

Wallace, J. M., and D. S. Gutzler, 1981: Teleconnections in the geopotential height field during the Northern Hemisphere winter. *Mon. Wea. Rev.*, **109,** 784–812.

——, C. Smith, and C. S. Bretherton, 1992: Singular value decomposition of wintertime sea surface temperature and 500-mb height anomalies. *J. Climate,* **5,** 561–576.

Wright, P. B., 1984: Relationships between indices of Southern Oscillation. *Mon. Wea. Rev.*, **112,** 1913–1919.

Zorita, E., V. Kharin, and H. v. Storch, 1992: The atmospheric circulation and sea surface temperature in the North Atlantic area in winter. Their interaction and relevance for Iberian precipitation. *J. Climate,* **5,** 1097–1108.